

# Novel Exact Traveling Wave Solutions for the (2 + 1)-Dimensional Boiti-Leon-Manna-Pempinelli Equation with Atangana's Space and Time Beta-Derivatives via the Sardar Subequation Method

Chanidaporn Pleumpreedaporn<sup>1</sup>, Songkran Pleumpreedaporn<sup>1,\*</sup>, Elvin J. Moore<sup>2,3</sup>,  
Sekson Sirisubtawee<sup>2,3</sup> and Surattana Sungnul<sup>2,3</sup>

<sup>1</sup> Department of Mathematics, Faculty of Science and Technology, Rambhai Barni Rajabhat University, Chanthaburi 22000, Thailand

e-mail : [chanidaporn.p@rbru.ac.th](mailto:chanidaporn.p@rbru.ac.th) (C. Pleumpreedaporn); [songkran.p@rbru.ac.th](mailto:songkran.p@rbru.ac.th) (S. Pleumpreedaporn)

<sup>2</sup> Department of Mathematics, Faculty of Applied Science, King Mongkut's University of Technology North Bangkok, Bangkok 10800, Thailand

e-mail : [elvin.j@sci.kmutnb.ac.th](mailto:elvin.j@sci.kmutnb.ac.th) (E.J. Moore); [sekson.s@sci.kmutnb.ac.th](mailto:sekson.s@sci.kmutnb.ac.th) (S. Sirisubtawee);  
[surattana.s@sci.kmutnb.ac.th](mailto:surattana.s@sci.kmutnb.ac.th) (S. Sungnul)

<sup>3</sup> Centre of Excellence in Mathematics, CHE, Si Ayutthaya Road, Bangkok 10400, Thailand

**Abstract** The (2 + 1)-dimensional Boiti-Leon-Manna-Pempinelli (BLMP) equation usually describes the interaction of a Riemann wave propagating along the  $y$ -axis with a long wave propagating along the  $x$ -axis. This equation can also be regarded as a generalization of a Kortewegde Vries (KdV) equation. In this paper, we generalize the BLMP equation by using Atangana's space and time beta-derivatives. We then use the Sardar subequation method and an appropriate traveling wave transformation to derive exact traveling wave solutions for the (2 + 1)-dimensional BLMP equation with fractional derivatives. The exact solutions of the equation are expressed in terms of generalized trigonometric and hyperbolic functions. These functions, which include both real- and complex-valued functions, are defined in this paper for the first time. Exact solutions are derived for a range of values of fractional orders and 2D, 3D and contour plots of the solutions are shown. Solutions are obtained for a range of parameter values to show some of the types of solution that can occur. As examples, we show solutions with physical behaviors such as a singular bell-shaped solitary wave solution, a solitary wave soliton of kink type and a periodic wave solution. We demonstrate that the proposed technique gives a straightforward and efficient method for deriving new exact traveling wave solutions for nonlinear partial differential equations such as the BLMP equation.

**MSC:** 35A25; 35G20; 35C07

**Keywords:** exact traveling wave solutions; Sardar subequation method; BLMP equation; Atangana's beta-derivative

---

Submission date: 02.06.2023 / Acceptance date: 31.08.2023

---

\*Corresponding author.

## 1. INTRODUCTION

Nonlinear evolution equations (NLEEs) are of importance because they are useful models for complex natural phenomena including, for example, behavior of shallow water waves [1] and properties of optical fiber soliton solutions of the nonlinear Schrödinger equation (NLSE) [2]. Recently, a variety of methods have been developed to derive exact solutions of NLEEs. These methods include an extended generalized  $(G'/G)$ -expansion method [3], the tanh-coth method [4], the F-expansion method [5], the Jacobi elliptic function method [6] and the Sardar subequation method [7].

In this paper, we focus on using the Sardar subequation method because it is a novel, powerful and productive approach for solving a range of NLEEs [7–10]. Two recent papers on the method and its applications that are closely related to our proposed work are as follows. Cina et al. [11] used the method to derive exact soliton solutions for the perturbed Fokas-Lenells (pFL) equation. Rezazadeh et al. [12] used the method to solve a variety of forms of  $(3 + 1)$ -dimensional Wazwaz-Benjamin-Bona-Mahony equations.

In particular, we are interested in using the method to obtain exact solutions of the  $(2 + 1)$ -dimensional Boiti-Leon-Manna-Pempinelli (BLMP) equation [13–15] which can be written in the form

$$b_{yt} + b_{xxx}y - 3(b_x b_{xy} + b_{xx} b_y) = 0, \quad (1.1)$$

where  $b = b(x, y, t)$ . Equation (1.1) was proposed by Gilson et al. [16] when they used the bilinear method to study a  $(2 + 1)$ -dimensional generalization of the Ablowitz, Kaup, Newell and Segur (AKNS) shallow-water wave equation. For this application, equation (1.1) shows the  $(2 + 1)$ -dimensional interaction of a shallow-water Riemann wave propagated along the  $y$ -axis with a shallow-water long wave propagated along the  $x$ -axis and  $b$  represents the vertical displacement of the water surface. Gilson et al. [16] showed that by replacing  $y = x$  in equation (1.1) and integrating the resulting equation the equation is reduced to a Kortewegde Vries (KdV) equation.

In this paper, we study a modified version of (1.1) in which the space and time partial derivatives are replaced by fractional space and time partial derivatives of Atangana's beta type [17, 18]. As is well known, the main reasons for introducing fractional derivatives are that they are expected to give improved models for systems with memory or hereditary properties (see, e.g. [19]). The definitions and usefulness of fractional derivatives will be explained in more detail in section 2. Then, the  $(2 + 1)$ -dimensional BLMP with Atangana's space and time beta-derivatives reads

$$\begin{aligned} & \frac{\partial^\alpha}{\partial t^\alpha} \left( \frac{\partial^\gamma b}{\partial y^\gamma} \right) + \frac{\partial^\gamma}{\partial y^\gamma} \left( \frac{\partial^\beta}{\partial x^\beta} \left( \frac{\partial^\beta}{\partial x^\beta} \left( \frac{\partial^\beta b}{\partial x^\beta} \right) \right) \right) \\ & - 3 \left( \frac{\partial^\beta b}{\partial x^\beta} \left( \frac{\partial^\gamma}{\partial y^\gamma} \left( \frac{\partial^\beta b}{\partial x^\beta} \right) \right) + \left( \frac{\partial^\beta}{\partial x^\beta} \left( \frac{\partial^\beta b}{\partial x^\beta} \right) \right) \right) \left( \frac{\partial^\gamma b}{\partial y^\gamma} \right) = 0, \end{aligned} \quad (1.2)$$

where, for a water wave,  $b$  usually represents a vertical surface displacement,  $\frac{\partial^\alpha}{\partial t^\alpha}(\cdot)$ ,  $\frac{\partial^\beta}{\partial x^\beta}(\cdot)$  and  $\frac{\partial^\gamma}{\partial y^\gamma}(\cdot)$  denote Atangana's partial beta-derivatives with respect to  $t$  of order  $0 < \alpha \leq 1$ , to  $x$  of order  $0 < \beta \leq 1$  and to  $y$  of order  $0 < \gamma \leq 1$ , respectively. The purpose of this study is to extract exact traveling wave solutions of equation (1.2) using the Sardar subequation method.

In section 2, we first give a brief description of Atangana’s beta-derivative [17, 18] and its important characteristics. We then discuss the algorithm of the Sardar subequation method [7]. In section 3, we describe the application of the Sardar subequation method to obtain exact solutions of Atangana’s beta-derivative BLMP equation (1.2). In section 4, we display graphs of selected exact solutions with their physical descriptions. Finally, a discussion of the results and conclusions are given in section 5.

## 2. PRELIMINARY CONCEPTS

### 2.1. ATANGANA’S BETA-DERIVATIVE AND ITS PROPERTIES

For ease of writing, in the remainder of this paper we will abbreviate Atangana’s beta-derivative to the commonly used beta fractional derivative or beta-derivative.

An advantage of fractional derivatives, such as the Caputo fractional derivative [19], the Riemann Liouville fractional derivative [19], the conformable derivative [20] and the beta-derivative [17, 18] is that they can be used to describe the properties of more general types of system than integer-order derivatives, especially if the system has memory or hereditary properties [19]. In this section, some important properties of the beta-derivative are defined and discussed. This derivative was initially proposed by Atangana et al. [17]. The beta-derivative can be studied as a natural extension of the classical derivative to a fractional order and most of its elementary properties are related to the elementary properties of classical derivatives.

**Definition 2.1.** Let  $f$  be a function such that  $f : [0, \infty) \rightarrow \mathbb{R}$ . Then, the beta-derivative of  $f$  of order  $\beta$ , where  $0 < \beta \leq 1$ , is defined by [17, 21–23]

$$D_t^\beta f(t) = \lim_{\varepsilon \rightarrow 0} \frac{f\left(t + \varepsilon \left(t + \frac{1}{\Gamma(\beta)}\right)^{1-\beta}\right) - f(t)}{\varepsilon}. \tag{2.1}$$

The basic properties of the beta-derivative are as follows [17, 18, 21, 23]. Let  $f(t), g(t)$  be  $\beta$ -differentiable functions for all  $t > 0$  and  $\beta \in (0, 1]$ . Then

- (1)  $D_t^\beta(\lambda) = 0, \forall \lambda \in \mathbb{R}$ .
- (2)  $D_t^\beta(af(t) + bg(t)) = aD_t^\beta f(t) + bD_t^\beta g(t), \forall a, b \in \mathbb{R}$ .
- (3)  $D_t^\beta(f(t)g(t)) = f(t)D_t^\beta g(t) + g(t)D_t^\beta f(t)$ .
- (4)  $D_t^\beta\left(\frac{f(t)}{g(t)}\right) = \frac{g(t)D_t^\beta f(t) - f(t)D_t^\beta g(t)}{(g(t))^2}$ , where  $g(t) \neq 0$ .
- (5) If  $f$  is differentiable, then  $D_t^\beta(f(t)) = \left(t + \frac{1}{\Gamma(\beta)}\right)^{1-\beta} \frac{df(t)}{dt}$ .

**Theorem 2.2** ([17, 18, 21, 24]). Suppose  $f, g : (0, \infty) \rightarrow \mathbb{R}$  are differentiable and also beta-differentiable. Further assume that  $g$  is a function defined in the range of  $f$ . Then, the beta-derivative of a composite function  $f \circ g$  can be written as

$$D_t^\beta(f \circ g)(t) = \left(t + \frac{1}{\Gamma(\beta)}\right)^{1-\beta} f'(g(t))g'(t), \tag{2.2}$$

where the prime symbol ( $'$ ) denotes the classical derivative.

By Definition 2.1, the beta partial derivative of a function  $u = u(x, t)$  with respect to  $t$  of order  $\beta \in (0, 1]$  can be defined by

$$\partial_t^\beta u(x, t) = \frac{\partial^\beta}{\partial t^\beta} u(x, t) = \lim_{\varepsilon \rightarrow 0} \frac{u\left(x, t + \varepsilon \left(t + \frac{1}{\Gamma(\beta)}\right)^{1-\beta}\right) - u(x, t)}{\varepsilon}, \quad t > 0. \quad (2.3)$$

In recent years, the beta-derivative has been used to solve a number of important problems in nonlinear PDEs. In [18], the beta-derivative was applied to obtain a magnetic soliton solution for periodic wave propagation of a Heisenberg ferromagnetic spin chain in a (2+1)-dimensional nonlinear Schrödinger equation (NLSE). The paper shows that the beta-derivative parameter significantly affects the rogue wave phenomena in this system and that the amplitudes and widths of such rogue waves are enlarged with the increase of  $\beta$ . The results are very helpful for analyzing the wave dynamics arising in many non-local and non-conservative/conservative physical systems. Another physical application of the  $\beta$ -derivative discussed in [22] involves the space-time fractional modified equal width (FMEW) equation. This equation is related to the regularized long wave (RLW) equation and has solitary wave solutions with both positive and negative amplitudes but the same width. In this study, new traveling wave solutions for the FMEW equation were constructed by using the unified method and varying the fractional-orders. The new solutions were expressed in both polynomial and rational forms. Further recent applications of the beta-derivative to physical systems include group velocity dispersion, unidirectional propagation of long waves and monomode optical fibers [21, 23, 25].

## 2.2. THE SARDAR SUBEQUATION METHOD

In order to apply the Sardar subequation method [7] to obtain solutions of nonlinear space-time partial differential equations with partial beta-derivatives, we must first transform the original problem into an ordinary differential equation (ODE) in a new variable  $\xi$ . The method is as follows. Consider the following nonlinear partial differential equation containing the partial beta-derivatives of a dependent variable  $u = u(x, y, t)$  with respect to independent variables  $x, y$  and  $t$ :

$$F_1(u, \partial_t^\alpha u, \partial_x^\beta u, \partial_y^\gamma u, \partial_t^\alpha (\partial_x^\beta u), \partial_t^\alpha (\partial_y^\gamma u), \partial_x^\beta (\partial_y^\gamma u), \dots) = 0, \quad 0 < \alpha, \beta, \gamma \leq 1, \quad (2.4)$$

where  $\partial_v^\gamma u = \frac{\partial^\gamma}{\partial v^\gamma} u$  is a generic term for the partial beta-derivative of the dependent variable  $u$  with respect to an independent variable  $v$  of order  $\gamma \in (0, 1]$ . The function  $F_1$  in equation (2.4) is assumed to be a polynomial of  $u$  and its various partial beta-derivatives. Then, applying the following fractional complex traveling wave transformation in a new variable  $\xi$  to equation (2.4), we obtain

$$u(x, y, t) = U(\xi), \quad \xi = \frac{k_1}{\beta} \left(x + \frac{1}{\Gamma(\beta)}\right)^\beta + \frac{k_2}{\gamma} \left(y + \frac{1}{\Gamma(\gamma)}\right)^\gamma + \frac{k_3}{\alpha} \left(t + \frac{1}{\Gamma(\alpha)}\right)^\alpha, \quad (2.5)$$

where  $k_1, k_2$  and  $k_3$  are nonzero constants which will be found at a later step. Then integrating the resulting equation with respect to  $\xi$  as many times as possible, we obtain an ODE in  $U = U(\xi)$  as

$$F_2(U, U', U'', U''', \dots) = 0, \quad (2.6)$$

where  $F_2$  is a polynomial function of  $U$  and its various integer-order derivatives. The prime notation ( $'$ ) denotes the ordinary derivative with respect to  $\xi$ .

Next, the Sardar subequation method [7–10] has the following main steps.

**STEP 1:** Assume that the exact solution of equation (2.6) is of the form

$$U(\xi) = \sum_{i=0}^N \omega_i \phi^i(\xi), \tag{2.7}$$

where  $\omega_i$ ,  $i = 0, 1, 2, \dots, N$  with  $\omega_N \neq 0$  are coefficients to be determined at a later step, and where the function  $\phi(\xi)$  satisfies the auxiliary equation

$$\phi'(\xi) = \sqrt{\rho + a\phi^2(\xi) + \phi^4(\xi)}, \tag{2.8}$$

with  $a$  and  $\rho$  being real constants to be determined at a later step.

The solutions of equation (2.8) are as follows:

*Case 1:* If  $a < 0$  and  $\rho = 0$ , then

$$\begin{aligned} \phi_1^\pm(\xi) &= \pm \sqrt{-mna} \operatorname{sec}_{mn}(\sqrt{-a}\xi), \\ \phi_2^\pm(\xi) &= \pm \sqrt{-mna} \operatorname{csc}_{mn}(\sqrt{-a}\xi). \end{aligned} \tag{2.9}$$

*Case 2:* If  $a > 0$  and  $\rho = 0$ , then

$$\begin{aligned} \phi_3^\pm(\xi) &= \pm \sqrt{-mna} \operatorname{sech}_{mn}(\sqrt{a}\xi), \\ \phi_4^\pm(\xi) &= \pm \sqrt{-mna} \operatorname{csch}_{mn}(\sqrt{a}\xi). \end{aligned} \tag{2.10}$$

*Case 3:* If  $a < 0$  and  $\rho = \frac{a^2}{4}$ , then

$$\begin{aligned} \phi_5^\pm(\xi) &= \pm \sqrt{-\frac{a}{2}} \operatorname{tanh}_{mn}\left(\sqrt{-\frac{a}{2}}\xi\right), \\ \phi_6^\pm(\xi) &= \pm \sqrt{-\frac{a}{2}} \operatorname{coth}_{mn}\left(\sqrt{-\frac{a}{2}}\xi\right), \\ \phi_7^\pm(\xi) &= \pm \sqrt{-\frac{a}{2}} \left( \operatorname{tanh}_{mn}(\sqrt{-2a}\xi) \pm i\sqrt{mn} \operatorname{sech}_{mn}(\sqrt{-2a}\xi) \right), \\ \phi_8^\pm(\xi) &= \pm \sqrt{-\frac{a}{2}} \left( \operatorname{coth}_{mn}(\sqrt{-2a}\xi) \pm \sqrt{mn} \operatorname{csch}_{mn}(\sqrt{-2a}\xi) \right), \\ \phi_9^\pm(\xi) &= \pm \sqrt{-\frac{a}{8}} \left( \operatorname{tanh}_{mn}\left(\sqrt{-\frac{a}{8}}\xi\right) + \operatorname{coth}_{mn}\left(\sqrt{-\frac{a}{8}}\xi\right) \right). \end{aligned} \tag{2.11}$$

*Case 4:* If  $a > 0$  and  $\rho = \frac{a^2}{4}$ , then

$$\begin{aligned} \phi_{10}^\pm(\xi) &= \pm \sqrt{\frac{a}{2}} \operatorname{tan}_{mn}\left(\sqrt{\frac{a}{2}}\xi\right), \\ \phi_{11}^\pm(\xi) &= \pm \sqrt{\frac{a}{2}} \operatorname{cot}_{mn}\left(\sqrt{\frac{a}{2}}\xi\right), \\ \phi_{12}^\pm(\xi) &= \pm \sqrt{\frac{a}{2}} \left( \operatorname{tan}_{mn}(\sqrt{2a}\xi) \pm \sqrt{mn} \operatorname{sec}_{mn}(\sqrt{2a}\xi) \right), \\ \phi_{13}^\pm(\xi) &= \pm \sqrt{\frac{a}{2}} \left( \operatorname{cot}_{mn}(\sqrt{2a}\xi) \pm \sqrt{mn} \operatorname{csc}_{mn}(\sqrt{2a}\xi) \right), \\ \phi_{14}^\pm(\xi) &= \pm \sqrt{\frac{a}{8}} \left( \operatorname{tan}_{mn}\left(\sqrt{\frac{a}{8}}\xi\right) - \operatorname{cot}_{mn}\left(\sqrt{\frac{a}{8}}\xi\right) \right), \end{aligned} \tag{2.12}$$

where

$$\begin{aligned} \sec_{mn}(\xi) &= \frac{2}{me^{i\xi} + ne^{-i\xi}}, & \csc_{mn}(\xi) &= \frac{2i}{me^{i\xi} - ne^{-i\xi}}, \\ \operatorname{sech}_{mn}(\xi) &= \frac{2}{me^\xi + ne^{-\xi}}, & \operatorname{csch}_{mn}(\xi) &= \frac{2i}{me^\xi - ne^{-\xi}}, \\ \tanh_{mn}(\xi) &= \frac{me^\xi - ne^{-\xi}}{me^\xi + ne^{-\xi}}, & \operatorname{coth}_{mn}(\xi) &= \frac{me^\xi + ne^{-\xi}}{me^\xi - ne^{-\xi}}, \\ \tan_{mn}(\xi) &= -i \frac{me^{i\xi} - ne^{-i\xi}}{me^{i\xi} + ne^{-i\xi}}, & \cot_{mn}(\xi) &= i \frac{me^{i\xi} + ne^{-i\xi}}{me^{i\xi} - ne^{-i\xi}} \end{aligned} \quad (2.13)$$

are special generalized trigonometric and hyperbolic functions. For more details, one can refer to [26–28].

**STEP 2:** Calculate the positive integer  $N$  in (2.7) using the homogeneous balance principle between the nonlinear terms and the highest order derivative appearing in equation (2.6). If we denote the degree of  $U(\xi)$  by  $\operatorname{Deg}[U(\xi)] = N$ , then the degree of other terms in the equation can be calculated by using the following formulas

$$\operatorname{Deg} \left[ \frac{d^q U(\xi)}{d\xi^q} \right] = N + q, \quad \operatorname{Deg} \left[ (U(\xi))^p \left( \frac{d^q U(\xi)}{d\xi^q} \right)^s \right] = Np + s(N + q). \quad (2.14)$$

**STEP 3:** Substituting equation (2.7) along with its required derivatives with the help of (2.8) into equation (2.6) and equating the coefficients of  $\phi^i(\xi)$  of the resulting polynomial to zero, we use the Maple software package to obtain a system of algebraic equations in  $\omega_i$  ( $i = 0, 1, \dots, N$ ),  $k_1, k_2$  and  $k_3$ .

**STEP 4:** The exact solutions of equation (2.4) can then be obtained by inserting the wave transformation (2.5) into the solution sets of equation (2.6).

### 3. APPLICATION OF THE METHOD

In this section, we apply the Sardar subequation method described in section 2 to obtain exact traveling wave solutions of equation (1.2). As explained in section 2, we must first convert equation (1.2) into an ordinary differential equation using the following transformation

$$b(x, y, t) = B(\xi), \quad \xi = \frac{p}{\beta} \left( x + \frac{1}{\Gamma(\beta)} \right)^\beta + \frac{q}{\gamma} \left( y + \frac{1}{\Gamma(\gamma)} \right)^\gamma + \frac{r}{\alpha} \left( t + \frac{1}{\Gamma(\alpha)} \right)^\alpha, \quad (3.1)$$

where  $p, q$  and  $r$  are nonzero constants which will be found at a later step. Substituting equation (3.1) into equation (1.2) and integrating the resulting equation with respect to  $\xi$  once, we obtain the following ODE in the variable  $B = B(\xi)$ :

$$p^3 q B''' - 3p^2 q (B')^2 + q r B' + K = 0, \quad (3.2)$$

where the prime notation ( $'$ ) represents the ordinary derivative with respect to  $\xi$  and  $K$  is a constant of integration. Based on equation (2.7), we assume that the solution form of (3.2) is

$$B(\xi) = \sum_{i=0}^N \omega_i \phi^i(\xi), \quad (3.3)$$

where  $\omega_i$ ,  $i = 1, 2, \dots, N$ , are constant coefficients and the function  $\phi(\xi)$  satisfies equation (2.8). Using the solution form (3.3) and the homogeneous balance principle, we

obtain  $N = 1$  and hence the solution of (3.2) is of the form

$$B(\xi) = \omega_0 + \omega_1 \phi(\xi), \tag{3.4}$$

where  $\omega_0$  and  $\omega_1$  will be determined through steps of the Sardar subequation method. Inserting (3.4) along with its required derivatives with the help of (2.8) into equation (3.2) and then equating the coefficients of  $\phi^i(\xi)$  (where  $i = 0, 1, 2, \dots, 8$ ) of the resulting polynomial to zero, we obtain the system of nonlinear algebraic equations in  $\omega_i$  ( $i = 0, 1$ ),  $p$ ,  $q$  and  $r$  with the help of the Maple software package as follows:

$$\begin{aligned} \phi^0 & : q^2 \omega_1^2 a^2 p^6 \rho - 9 p^4 q^2 \omega_1^4 \rho^2 + 2 q^2 \omega_1^2 a p^3 r \rho + 6 p^2 q \omega_1^2 \rho K + q^2 \omega_1^2 r^2 \rho - K^2 = 0, \\ \phi^2 & : a^3 p^6 q^2 \omega_1^2 + 12 a p^6 q^2 \rho \omega_1^2 - 18 a p^4 q^2 \rho \omega_1^4 + 2 a^2 p^3 q^2 r \omega_1^2 + 12 p^3 q^2 r \rho \omega_1^2 \\ & \quad + 6 K a p^2 q \omega_1^2 + a q^2 r^2 \omega_1^2 = 0, \\ \phi^4 & : 13 a^2 p^6 q^2 \omega_1^2 - 9 a^2 p^4 q^2 \omega_1^4 + 36 p^6 q^2 \rho \omega_1^2 - 18 p^4 q^2 \rho \omega_1^4 + 14 a p^3 q^2 r \omega_1^2 \\ & \quad + 6 K p^2 q \omega_1^2 + q^2 r^2 \omega_1^2 = 0, \\ \phi^6 & : 48 a p^6 q^2 \omega_1^2 - 18 a p^4 q^2 \omega_1^4 + 12 p^3 q^2 r \omega_1^2 = 0, \\ \phi^8 & : 36 p^6 q^2 \omega_1^2 - 9 p^4 q^2 \omega_1^4 = 0. \end{aligned} \tag{3.5}$$

Unfortunately, the coefficients of  $\phi^i(\xi)$  are zero when  $i$  is odd, so their equations are not shown in system (3.5). Using the Maple 17 software package to solve system (3.5), we obtain only one set of solutions as follows:

$$\omega_0 = \omega_0, \omega_1 = \pm 2p, K = 0, p = p, q = q, r = 2p^3 a, \rho = \frac{a^2}{4}, \tag{3.6}$$

where  $\omega_0, p, q$  and  $a$  are arbitrary constants with  $p, q \neq 0$ . In consequence, the exact solutions of equation (3.4) corresponding to equation (3.6) along with equations (2.9)-(2.12) are as follows.

*Case 1:* If  $a < 0$  and  $\rho = 0$ , then there are no exact solutions  $b_{1,2}^\pm(x, y, t)$  because, by (3.6), if  $\rho = 0$ , then  $a$  must be zero, which contradicts the condition that  $a < 0$ .

*Case 2:* If  $a > 0$  and  $\rho = 0$ , then there are no exact solutions  $b_{3,4}^\pm(x, y, t)$  because, by (3.6), if  $\rho = 0$ , then  $a$  must be zero, which contradicts the condition that  $a > 0$ .

From (3.6), we have  $\rho = \frac{a^2}{4}$ . Therefore, by the Sardar subequation method and algebraic manipulations, we have that the only solutions of (3.4) are as follows.

*Case 3:* If  $a < 0$  and  $\rho = \frac{a^2}{4}$ , then the exact traveling wave solutions are

$$b_5(x, y, t) = \omega_0 - 2p \sqrt{-\frac{a}{2}} \tanh_{mn} \left( \sqrt{-\frac{a}{2}} \xi \right), \tag{3.7}$$

$$b_6(x, y, t) = \omega_0 - 2p \sqrt{-\frac{a}{2}} \coth_{mn} \left( \sqrt{-\frac{a}{2}} \xi \right), \tag{3.8}$$

$$b_7^\pm(x, y, t) = \omega_0 - 2p \sqrt{-\frac{a}{2}} \left( \tanh_{mn}(\sqrt{-2a}\xi) \pm i \sqrt{mn} \operatorname{sech}_{mn}(\sqrt{-2a}\xi) \right), \tag{3.9}$$

$$b_8^\pm(x, y, t) = \omega_0 - 2p \sqrt{-\frac{a}{2}} \left( \coth_{mn}(\sqrt{-2a}\xi) \pm \sqrt{mn} \operatorname{csch}_{mn}(\sqrt{-2a}\xi) \right), \tag{3.10}$$

$$b_9(x, y, t) = \omega_0 - 2p\sqrt{-\frac{a}{8}} \left( \tanh_{mn} \left( \sqrt{-\frac{a}{8}}\xi \right) + \coth_{mn} \left( \sqrt{-\frac{a}{8}}\xi \right) \right), \quad (3.11)$$

where

$$\xi = \frac{p}{\beta} \left( x + \frac{1}{\Gamma(\beta)} \right)^\beta + \frac{q}{\gamma} \left( y + \frac{1}{\Gamma(\gamma)} \right)^\gamma + \frac{2p^3a}{\alpha} \left( t + \frac{1}{\Gamma(\alpha)} \right)^\alpha. \quad (3.12)$$

*Case 4:* If  $a > 0$  and  $\rho = \frac{a^2}{4}$ , then the exact traveling wave solutions are

$$b_{10}(x, y, t) = \omega_0 + 2p\sqrt{\frac{a}{2}} \tan_{mn} \left( \sqrt{\frac{a}{2}}\xi \right), \quad (3.13)$$

$$b_{11}(x, y, t) = \omega_0 - 2p\sqrt{\frac{a}{2}} \cot_{mn} \left( \sqrt{\frac{a}{2}}\xi \right), \quad (3.14)$$

$$b_{12}^\pm(x, y, t) = \omega_0 + 2p\sqrt{\frac{a}{2}} \left( \tan_{mn} \left( \sqrt{2a}\xi \right) \pm \sqrt{mn} \sec_{mn} \left( \sqrt{2a}\xi \right) \right), \quad (3.15)$$

$$b_{13}^\pm(x, y, t) = \omega_0 - 2p\sqrt{\frac{a}{2}} \left( \cot_{mn} \left( \sqrt{2a}\xi \right) \pm \sqrt{mn} \csc_{mn} \left( \sqrt{2a}\xi \right) \right), \quad (3.16)$$

$$b_{14}(x, y, t) = \omega_0 + 2p\sqrt{\frac{a}{8}} \left( \tan_{mn} \left( \sqrt{\frac{a}{8}}\xi \right) - \cot_{mn} \left( \sqrt{\frac{a}{8}}\xi \right) \right), \quad (3.17)$$

where

$$\xi = \frac{p}{\beta} \left( x + \frac{1}{\Gamma(\beta)} \right)^\beta + \frac{q}{\gamma} \left( y + \frac{1}{\Gamma(\gamma)} \right)^\gamma + \frac{2p^3a}{\alpha} \left( t + \frac{1}{\Gamma(\alpha)} \right)^\alpha. \quad (3.18)$$

We have checked that the functions in equations (3.7) to (3.17) are exact solutions of the original equation (1.2) by substituting them in Maple 17 and finding that they satisfy equation (1.2).

#### 4. GRAPHICAL REPRESENTATIONS OF SOME SOLUTIONS

In this section, we show graphs of some interesting exact traveling wave solutions of the beta-derivative  $(2 + 1)$ -dimensional BLMP equation (1.2). In particular, the exact traveling wave solutions  $b_5(x, y, t)$  in equation (3.7),  $b_7^\pm(x, y, t)$  in equation (3.9), and  $b_{14}(x, y, t)$  in equation (3.17) have been selected to show the type of solution and how their physical behavior changes when values of the fractional-orders  $\alpha, \beta, \gamma$  are varied. For each solution, the magnitudes of the exact solutions are shown as 3D, 2D and contour plots for the following range of fractional-order values:  $\alpha = 1, 0.8, 0.6$ ,  $\beta = 1, 0.9, 0.6$  and  $\gamma = 1, 0.8$ . In all cases, the 3D, 2D graphs and the contour plots representing a 3D surface by plotting  $(x, t)$  contours for a range of fixed magnitude values of the selected solutions are portrayed using the Maple software package.

In Figures 1–3, magnitudes of the exact solution  $b_5(x, y, t)$  in (3.7) are plotted as 3D on the domain  $D_1 = \{(x, y, t) | 0 \leq x \leq 1, y = 1 \text{ and } -1 \leq t \leq 1\}$ , 2D on the domain  $D_2 = \{(x, y, t) | x = y = 1, -1 \leq t \leq 1\}$  and contour plots for the following parameter

values:  $a = -1$ ,  $m = 1.2$ ,  $n = 1.4$ ,  $p = 2$ ,  $q = 3$ ,  $\omega_0 = 0.5$ ,  $K = 0$ . Figures 1 (a)-(c) show the 3D, 2D and contour plots for the magnitude of the exact solution  $b_5(x, y, t)$  calculated at the following set of integer orders:  $\{\alpha = 1, \beta = 1, \gamma = 1\}$ . Figures 2 (a)-(c), (d)-(f) and (g)-(i) show the 3D, 2D and contour plots for the magnitude of the exact solution  $b_5(x, y, t)$  calculated at the following sets of fractional orders  $\{\alpha = 1, \beta = 0.9, \gamma = 0.8\}$ ,  $\{\alpha = 0.8, \beta = 0.9, \gamma = 0.8\}$  and  $\{\alpha = 0.6, \beta = 0.9, \gamma = 0.8\}$ , respectively. Figures 3 (a)-(c), (d)-(f) and (g)-(i) show the 3D, 2D and contour plots for the magnitude of the exact solution  $b_5(x, y, t)$  calculated at the following sets  $\{\alpha = 1, \beta = 0.6, \gamma = 0.8\}$ ,  $\{\alpha = 0.8, \beta = 0.6, \gamma = 0.8\}$  and  $\{\alpha = 0.6, \beta = 0.6, \gamma = 0.8\}$ , respectively. As can be seen from the 3D graphs of Figures 1-3, the physical behavior of  $|b_5(x, y, t)|$  can be classified as a singular bell-shaped solitary wave. It can also be seen that the main effect of changing the fractional orders is to move the positions of the singularities in the solitary waves.

In Figures 4-6, magnitudes of the exact solution  $b_7^+(x, y, t)$  in (3.9) are plotted as 3D on the domain  $D_3 = \{(x, y, t) | 0 \leq x \leq 10, y = 1 \text{ and } -3 \leq t \leq 3\}$ , 2D on the domain  $D_4 = \{(x, y, t) | x = y = 1, -3 \leq t \leq 3\}$  and contour plots for the following parameter values:  $a = -1$ ,  $m = 1.2$ ,  $n = 1.4$ ,  $p = 2$ ,  $q = 3$ ,  $\omega_0 = 0.5$ ,  $K = 0$ . Figures 4 (a)-(c) show the 3D, 2D and contour plots for the magnitude of the exact solution  $b_7^+(x, y, t)$  calculated at the following set of integer orders:  $\{\alpha = 1, \beta = 1, \gamma = 1\}$ . Figures 5 (a)-(c), (d)-(f) and (g)-(i) show the 3D, 2D and contour plots for the magnitude of the exact solution  $b_7^+(x, y, t)$  calculated at the following sets of fractional orders  $\{\alpha = 1, \beta = 0.9, \gamma = 0.8\}$ ,  $\{\alpha = 0.8, \beta = 0.9, \gamma = 0.8\}$  and  $\{\alpha = 0.6, \beta = 0.9, \gamma = 0.8\}$ , respectively. Figures 6 (a)-(c), (d)-(f) and (g)-(i) show the 3D, 2D and contour plots for the magnitude of the exact solution  $b_7^+(x, y, t)$  calculated at the following sets  $\{\alpha = 1, \beta = 0.6, \gamma = 0.8\}$ ,  $\{\alpha = 0.8, \beta = 0.6, \gamma = 0.8\}$  and  $\{\alpha = 0.6, \beta = 0.6, \gamma = 0.8\}$ , respectively. As can be seen from the 3D and 2D graphs of Figures 4-6, the physical behavior of  $|b_7^+(x, y, t)|$  can be characterized as a solitary wave soliton of kink type. It can also be seen that the main effect of changing the fractional orders is to move the position of the kink in the solitary wave soliton.

In Figures 7-9, magnitudes of the exact solution  $b_{14}(x, y, t)$  in (3.17) are plotted as 3D on the domain  $D_5 = \{(x, y, t) | 0 \leq x \leq 1, y = 1 \text{ and } 0 \leq t \leq 1\}$ , 2D on  $D_6 = \{(x, y, t) | x = y = 1, 0 \leq t \leq 1\}$  and contour plots for the following parameter values:  $a = -1$ ,  $m = 1.2$ ,  $n = 1.4$ ,  $p = 2$ ,  $q = 3$ ,  $\omega_0 = 0.5$ ,  $K = 0$ . Figures 7 (a)-(c) show the 3D, 2D and contour plots for the magnitude of the exact solution  $b_{14}(x, y, t)$  calculated at the following set of integer orders:  $\{\alpha = 1, \beta = 1, \gamma = 1\}$ . Figures 8 (a)-(c), (d)-(f) and (g)-(i) show the 3D, 2D and contour plots for the magnitude of the exact solution  $b_{14}(x, y, t)$  calculated at the following sets of fractional orders  $\{\alpha = 1, \beta = 0.9, \gamma = 0.8\}$ ,  $\{\alpha = 0.8, \beta = 0.9, \gamma = 0.8\}$  and  $\{\alpha = 0.6, \beta = 0.9, \gamma = 0.8\}$ , respectively. Figures 9 (a)-(c), (d)-(f) and (g)-(i) show the 3D, 2D and contour plots for the magnitude of the exact solution  $b_{14}(x, y, t)$  calculated at the following sets  $\{\alpha = 1, \beta = 0.6, \gamma = 0.8\}$ ,  $\{\alpha = 0.8, \beta = 0.6, \gamma = 0.8\}$  and  $\{\alpha = 0.6, \beta = 0.6, \gamma = 0.8\}$ , respectively. From the 3D graphs of Figures 7-9, the physical behavior of  $|b_{14}(x, y, t)|$  can be characterized as a periodic wave solution. It can also be seen that the main effect of changing the fractional orders is to change the periods of the solution.

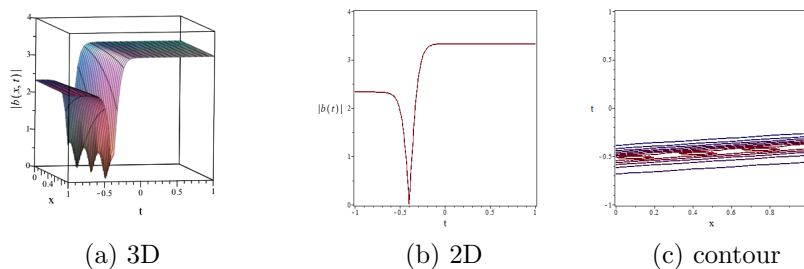


FIGURE 1. Graphs of magnitudes for  $b_5(x, y, t)$  in (3.7) obtained utilizing the Sardar subequation method: (a)-(c)  $\alpha = 1, \beta = 1, \gamma = 1$ .

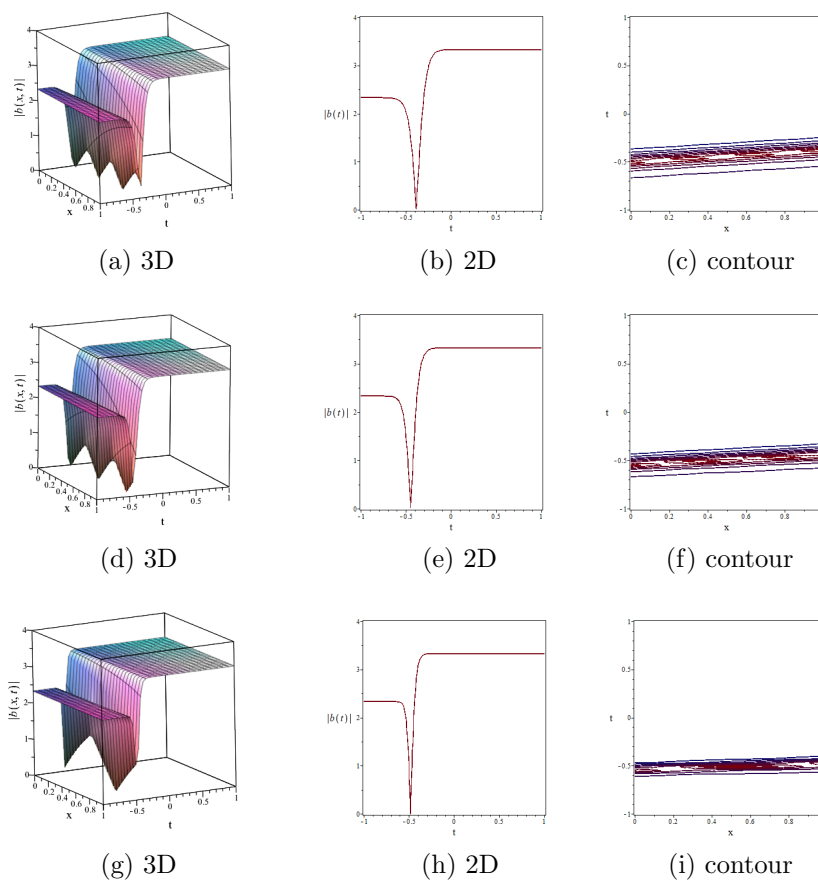


FIGURE 2. Graphs of magnitudes for  $b_5(x, y, t)$  in (3.7) obtained utilizing the Sardar subequation method: (a)-(c)  $\alpha = 1, \beta = 0.9, \gamma = 0.8$ ; (d)-(f)  $\alpha = 0.8, \beta = 0.9, \gamma = 0.8$ ; (g)-(i)  $\alpha = 0.6, \beta = 0.9, \gamma = 0.8$ .

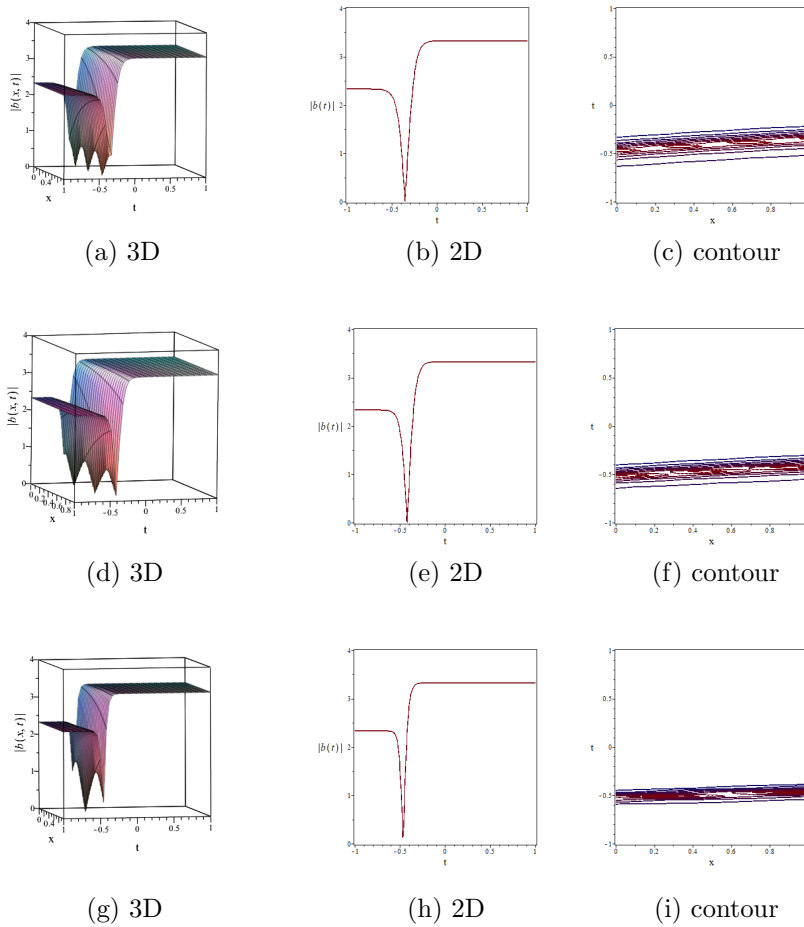


FIGURE 3. Graphs of magnitudes for  $b_5(x, y, t)$  in (3.7) obtained utilizing the Sardar subequation method: (a)-(c)  $\alpha = 1, \beta = 0.6, \gamma = 0.8$ ; (d)-(f)  $\alpha = 0.8, \beta = 0.6, \gamma = 0.8$ ; (g)-(i)  $\alpha = 0.6, \beta = 0.6, \gamma = 0.8$ .

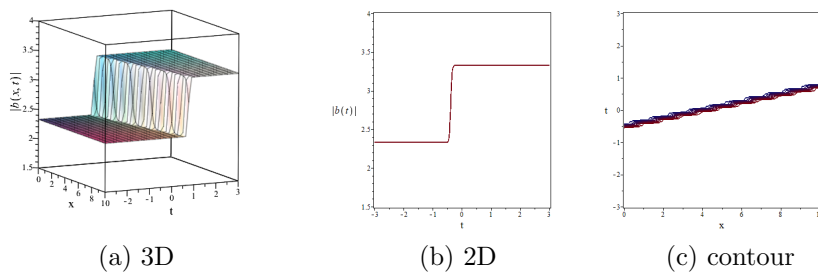


FIGURE 4. Graphs of magnitudes for  $b_7^+(x, y, t)$  in (3.9) obtained utilizing the Sardar subequation method: (a)-(c)  $\alpha = 1, \beta = 1, \gamma = 1$ .

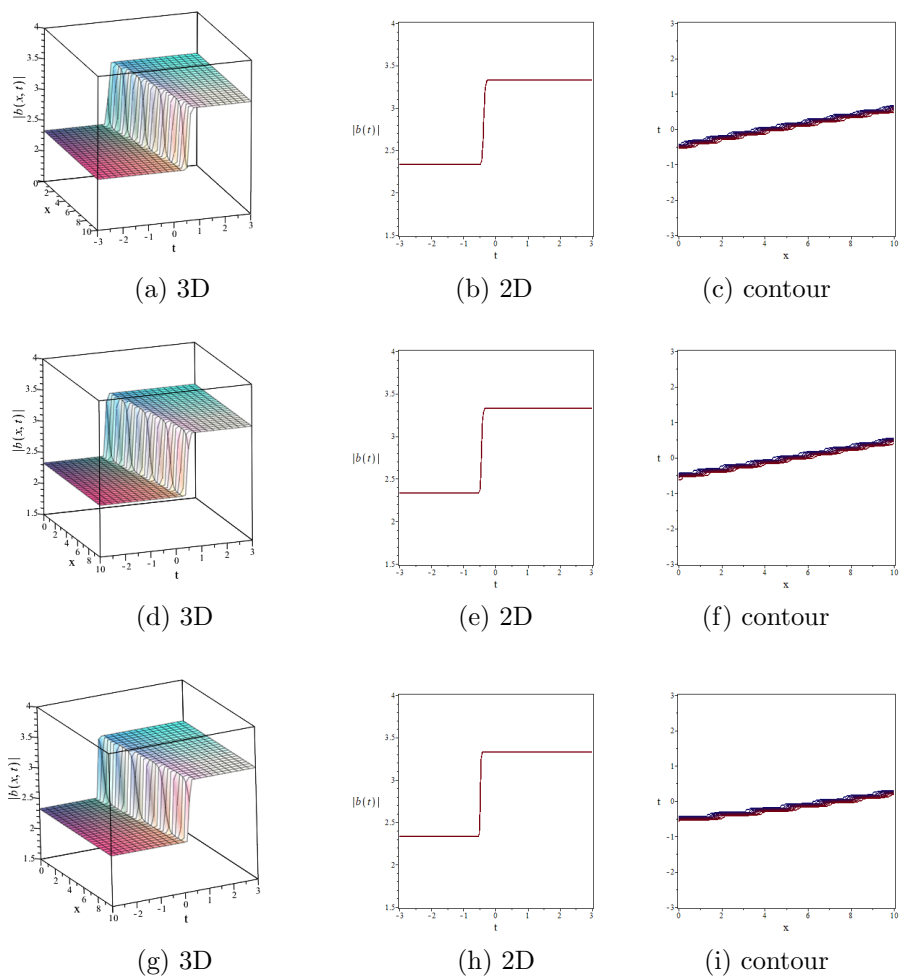


FIGURE 5. Graphs for magnitudes of  $b_r^+(x, y, t)$  in (3.9) obtained using the Sardar subequation method: (a)-(c)  $\alpha = 1$ ,  $\beta = 0.9$ ,  $\gamma = 0.8$ ; (d)-(f)  $\alpha = 0.8$ ,  $\beta = 0.9$ ,  $\gamma = 0.8$ ; (g)-(i)  $\alpha = 0.6$ ,  $\beta = 0.9$ ,  $\gamma = 0.8$ .

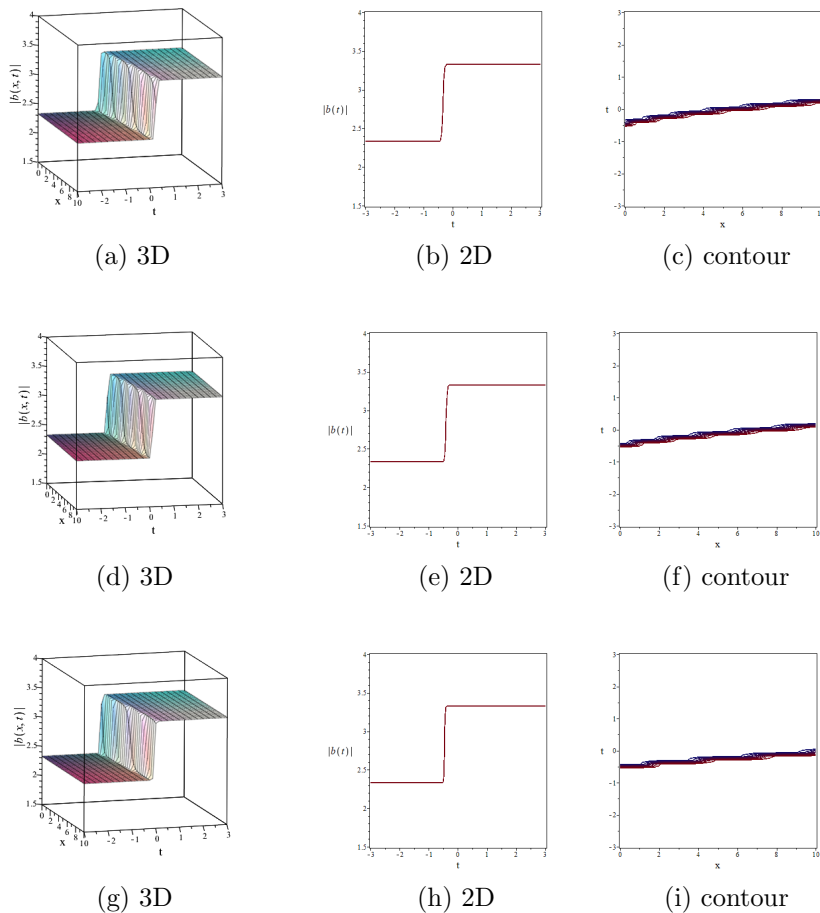


FIGURE 6. Graphs of magnitudes for  $b_7^+(x, y, t)$  in (3.9) obtained utilizing the Sardar subequation method: (a)-(c)  $\alpha = 1, \beta = 0.6, \gamma = 0.8$ ; (d)-(f)  $\alpha = 0.8, \beta = 0.6, \gamma = 0.8$ ; (g)-(i)  $\alpha = 0.6, \beta = 0.6, \gamma = 0.8$ .

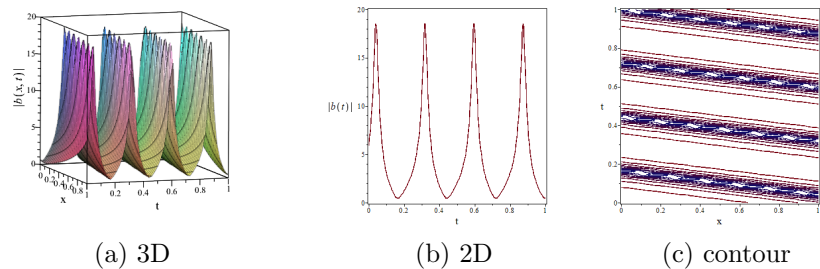


FIGURE 7. Graphs of magnitudes for  $b_{14}(x, y, t)$  in (3.17) obtained utilizing the Sardar subequation method: (a)-(c)  $\alpha = 1, \beta = 1, \gamma = 1$ .

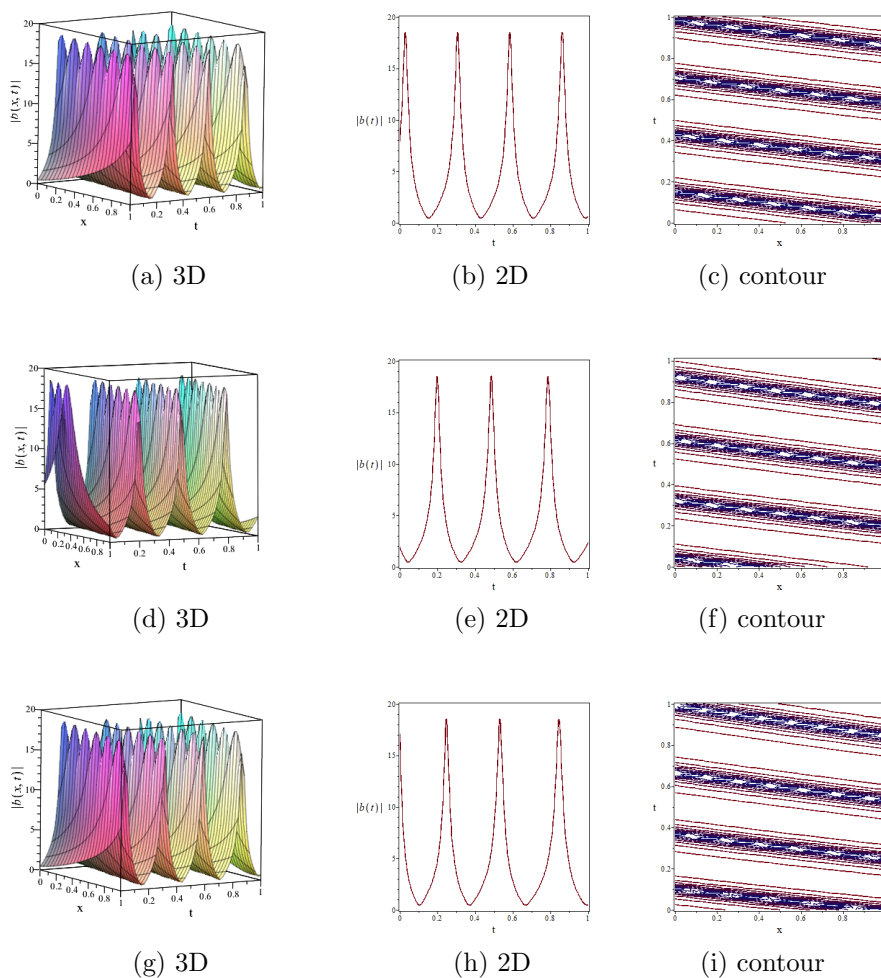


FIGURE 8. Graphs for magnitudes of  $b_{14}(x, y, t)$  in (3.17) obtained using the Sardar subequation method: (a)-(c)  $\alpha = 1, \beta = 0.9, \gamma = 0.8$ ; (d)-(f)  $\alpha = 0.8, \beta = 0.9, \gamma = 0.8$ ; (g)-(i)  $\alpha = 0.6, \beta = 0.9, \gamma = 0.8$ .

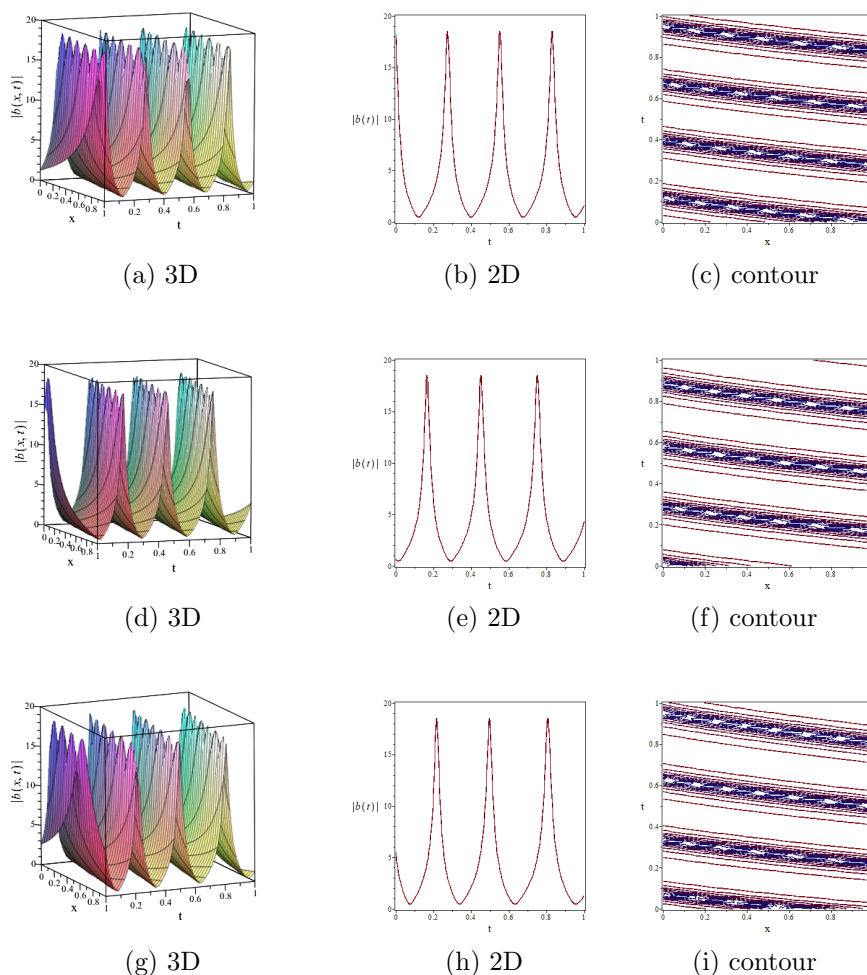


FIGURE 9. Graphs of magnitudes for  $b_{14}(x, y, t)$  in (3.17) obtained utilizing the Sardar subequation method: (a)-(c)  $\alpha = 1, \beta = 0.6, \gamma = 0.8$ ; (d)-(f)  $\alpha = 0.8, \beta = 0.6, \gamma = 0.8$ ; (g)-(i)  $\alpha = 0.6, \beta = 0.6, \gamma = 0.8$ .

### 5. CONCLUSIONS

In this research, the Sardar subequation method has been used to obtain exact traveling wave solutions of the (2 + 1)-dimensional BLMPE equation (1.2) with Atangana’s space and time beta-derivatives. Using this method, and with the aid of the Maple 17 software package, we have successfully found exact solutions of the equation in terms of the special generalized trigonometric and hyperbolic functions defined in (2.13). The exact solutions obtained in this paper have not been reported by any previous authors. Further, the Maple package has been used to plot 3D, 2D and contour plots of the magnitude of

selected solutions for a range of values of fractional-orders  $\alpha$ ,  $\beta$  and  $\gamma$  in order to explore their effects on the physical behavior of selected solutions. From the results, we have selected three of the exact solutions of equation (1.2) with different physical behaviors, namely, a singular bell-shaped solitary wave solution, a solitary wave soliton of kink type, and a periodic wave solution. As stated at the end of section 3, we have verified that all of the solutions in section 3 are exact solutions of equation (1.2) by substituting them back into the original equation with the assistance of Maple. In conclusion, we believe that the Sardar subequation method is a powerful and reliable technique for obtaining exact traveling wave solutions of integer-order and fractional order nonlinear evolution equations of the BLMP type. The aim of this paper has been to show that the Sardar subequation method is a useful method for obtaining exact solutions of nonlinear evolution equations of the BLMP type with fractional order beta-derivatives. Possible future work would be to compare the fractional model and solutions obtained in this paper with data from real physical systems.

## ACKNOWLEDGEMENTS

The authors are grateful to anonymous referees for the valuable comments which have significantly improved this article. In addition, the first and second authors are financially supported by the Department of Mathematics, Faculty of Science and Technology, Rambhai Barni Rajabhat University, Chanthaburi.

## REFERENCES

- [1] Y. Gu, S.M. Zia, M. Isam, J. Manafian, A. Hajar, M. Abotaleb, Bilinear method and semi-inverse variational principle approach to the generalized (2+1)-dimensional shallow water wave equation, *Results in Physics* 45 (2023) 106213.
- [2] H.A. Mardi, N. Nasaruddin, M. Ikhwan, N. Nurmaulidar, M. Ramli, Soliton dynamics in optical fiber based on nonlinear Schrödinger equation, *Heliyon* 9 (3) (2023) 1–15.
- [3] S.K. Mohanty, O.V. Kravchenko, M.K. Deka, A.N. Dev, D.V. Churikov, The exact solutions of the (2+1)-dimensional Kadomtsev–Petviashvili equation with variable coefficients by extended generalized ( $G'/G$ )-expansion method, *Journal of King Saud University-Science* 35 (1) (2023) 102358.
- [4] S. Naowarat, S. Saifullah, S. Ahmad, M. De la Sen, Periodic, singular and dark solitons of a generalized geophysical KdV equation by using the tanh-coth method, *Symmetry* 15 (1) (2023) 1–10.
- [5] M. Ozisik, A. Secer, M. Bayram, On solitary wave solutions for the extended nonlinear Schrödinger equation via the modified F-expansion method, *Optical and Quantum Electronics* 55 (3) (2023) 1–23.
- [6] T.A. Khalil, N. Badra, H.M. Ahmed, W.B. Rabie, Optical solitons and other solutions for coupled system of nonlinear Biswas–Milovic equation with Kudryashov’s law of refractive index by Jacobi elliptic function expansion method, *Optik* 253 (2022) 168540.
- [7] R. Hussain, A. Imtiaz, T. Rasool, H. Rezazadeh, M. İnç, Novel exact and solitary solutions of conformable Klein–Gordon equation via Sardar-subequation method, *Journal of Ocean Engineering and Science* (2022) 1–7.

- 
- [8] M.I. Asjad, M. Inc, I. Iqbal, Exact solutions for new coupled Konno–Oono equation via Sardar subequation method, *Optical and Quantum Electronics* 54 (12) (2022) 1–16.
- [9] H.U. Rehman, I. Iqbal, S. Subhi Aiadi, N. Mlaiki, M.S. Saleem, Soliton solutions of Klein–Fock–Gordon equation using Sardar subequation method, *Mathematics* 10 (18) (2022) 1–10.
- [10] H.U. Rahman, M.I. Asjad, N. Munawar, F. Parvaneh, T. Muhammad, A.A. Hamoud, H. Emadifar, F.K. Hamasalh, H. Azizi, M. Khademi, Traveling wave solutions to the Boussinesq equation via Sardar sub-equation technique, *AIMS Mathematics* 7 (6) (2022) 11134–11149.
- [11] M. Cinar, A. Secer, M. Ozisik, M. Bayram, Derivation of optical solitons of dimensionless Fokas–Lenells equation with perturbation term using Sardar subequation method, *Optical and Quantum Electronics* 54 (7) (2022) 1–13.
- [12] H. Rezazadeh, M. Inc, D. Baleanu, New solitary wave solutions for variants of (3+1)-dimensional Wazwaz–Benjamin–Bona–Mahony equations, *Frontiers in Physics* 8 (2020) 1–11.
- [13] N. Mahak, G. Akram, A family of novel exact solutions to (2+1)-dimensional Boiti–Leon–Manna–Pempinelli equation, *Authorea Preprints* (2020) 1–10.
- [14] Y. Li, D. Li, New exact solutions for the (2+1)-dimensional Boiti–Leon–Manna–Pempinelli equation, *Applied Mathematical Sciences* 6 (2012) 579–587.
- [15] S. Mabrouk, M. Kassem, Group similarity solutions of (2+1) Boiti–Leon–Manna–Pempinelli Lax pair, *Ain Shams Engineering Journal* 5 (1) (2014) 227–235.
- [16] C. Gilson, J. Nimmo, R. Willox, A (2+1)-dimensional generalization of the AKNS shallow water wave equation, *Physics Letters A* 180 (4) (1993) 337–345.
- [17] A. Atangana, D. Baleanu, A. Alsaedi, Analysis of time-fractional Hunter–Saxton equation: A model of neumatic liquid crystal, *Open Physics* 14 (1) (2016) 145–149.
- [18] M.F. Uddin, M.G. Hafez, Z. Hammouch, D. Baleanu, Periodic and rogue waves for Heisenberg models of ferromagnetic spin chains with fractional beta derivative evolution and obliqueness, *Waves in Random and Complex Media* 31 (6) (2021) 2135–2149.
- [19] I. Podlubny, *Fractional Differential Equations*, Academic Press, San Diego, 1999.
- [20] R. Khalil, M. Al Horani, A. Yousef, M. Sababheh, A new definition of fractional derivative, *Journal of Computational and Applied Mathematics* 264 (2014) 65–70.
- [21] E.M. Ozkan, New exact solutions of some important nonlinear fractional partial differential equations with beta derivative, *Fractal and Fractional* 6 (3) (2022) 1–11.
- [22] M.N. Rafiq, A. Majeed, M. Inc, M. Kamran, New traveling wave solutions for space-time fractional modified equal width equation with beta derivative, *Physics Letters A* 446 (2022) 128281.
- [23] A. Akbulut, S. Islam, Study on the Biswas–Arshed equation with the beta time derivative, *International Journal of Applied and Computational Mathematics* 8 (4) (2022) 1–13.

- [24] X.Z. Zhang, M.N. Rafiq, A. Majeed, M. Inc, M. Kamran, New traveling wave solutions for space-time fractional modified equal width equation with beta derivative, *Physics Letters A* 446 (2022) 128281.
- [25] K. Hosseini, M. Mirzazadeh, J. Gómez-Aguilar, Soliton solutions of the Sasa-Satsuma equation in the monomode optical fibers including the beta-derivatives, *Optik* 224 (2020) 165425.
- [26] H. Miyakawa, S. Takeuchi, Applications of a duality between generalized trigonometric and hyperbolic functions, *Journal of Mathematical Analysis and Applications* 502 (1) (2021) 125241.
- [27] G. Dattoli, S. Licciardi, R.M. Pidotella, Theory of generalized trigonometric functions: From Laguerre to Airy forms, *Journal of Mathematical Analysis and Applications* 468 (1) (2018) 103–115.
- [28] M.K. Elboree, Hyperbolic and trigonometric solutions for some nonlinear evolution equations, *Communications in Nonlinear Science and Numerical Simulation* 17 (11) (2012) 4085–4096.